Electronic Supplementary Information

Lithium–oxygen batteries with triplex Li^+-selective solid membranes

Youngbin Choi [a], Keeyoung Jung [b], Hyeong-Jun Kim [a], Ji-Woong Moon [b,*], Jong-Won Lee [a,*]

[a] *Department of Materials Science and Engineering, Chosun University, 309 Pilmun-daero, Dong-gu, Gwangju 61452, Republic of Korea*

[b] *Materials Research Division, Research Institute of Industrial Science and Technology, Pohang 37673, Republic of Korea*

* Corresponding author

E-mail: jongwon@chosun.ac.kr (J.-W. Lee), jwmoon@rist.re.kr (J.-W. Moon)

Preparation of triplex-LSSMs

A triplex LSSM was fabricated via tape casting as follows. A slurry was prepared by mixing $Li_{1+x+y}Al_xTi_{2-x}Si_yP_{3-y}O_{12}$ (LATP) powder (average particle size = 0.4 μm, LICGC™-PW-01 OHARA Inc., Japan) and BYK111 (dispersant) in toluene and isopropanol. After ball milling for 18 h, polyvinyl butyral (binder) and dioctyl phthalate (plasticizer) were added to the slurry, followed by ball milling for 18 h. The milling and mixing were conducted using a laboratory ball mill (Samhung Energy Ltd.) and yttria-stabilized tetragronal zirconia balls (diameter = 10 mm (50 wt%) and 5 mm (50 wt%)) at 100 rpm. The slurry was degassed via stirring in a vacuum chamber for 3 h and then coated on a Mylar film. The resulting green tape was dried at 50 ^oC for 2 h. To fabricate a porous tape, polymethyl methacrylate (PMMA) beads (pore-former) with a diameter of 5 μm were added to the well-mixed slurry before the degassing process. The green tape was laminated together via warm-isostatic pressing at 1,500 psi and 65 ^oC for 30 min to form a triplex (porous/dense/porous) structure. The laminated tape was cut into a disk with a diameter of 28 mm, heat-treated in air at 500 ^oC (ramp rate = 0.15 ^oC min^{-1}) for 6 h to remove organic components, and finally co-sintered in air at 1,025 ^oC (ramp rate = 0.45 ^oC min^{-1}) for 4 h.

Material characterizations

The phase and crystal structure of the prepared solid membranes were characterized via X-ray diffraction (XRD) analysis. An automated Rigaku diffractometer (2500 D/MAX, Rigaku) with Cu K_α radiation was used for the XRD measurements. Microstructural analysis was performed using scanning electron microscopy (SEM, Hitachi X–4900). To examine the sinterability and perform electrical characterization, the LATP powders were pressed into a disk under a pressure of 400 MPa and then sintered at 1,025 ^oC for 4 h in air. The relative density of the sintered sample was estimated using Archimedes' method. To measure the Li^+ conductivity, both sides of the LATP pellet were sputtered with Au (ion-blocking electrode), and then the AC-impedance spectra were measured in the frequency (f) range of 10^{-1} to 10^6 Hz with an AC signal amplitude of 5 mV using a Bio-Logic SP-200.

Electrochemical experiments

An LOB cell was constructed using a specially designed two-compartment cell and was composed of a Li metal anode, triplex-LSSM, and a carbon cathode. The anolyte was 1 M $LiPF_6$ dissolved in a mixed solvent of ethylene carbonate (EC) and ethylmethyl carbonate (EMC) (3:7 by volume), and the catholyte was 1 M Li bis(trifluoromethane-sulfonyl)imide (LiTFSI) in tetraethylene glycol dimethyl ether (TEGDME). The catholyte was directly impregnated into the porous LSSM layer without using an additional separator, whereas a porous glass fiber separator was placed on the anode side to avoid the side reaction of LATP with Li . The cathode was prepared as a thin sheet of carbon nanotubes (CNTs) (buckypaper) with a fibrous morphology and a macroporous structure. For the preparation of CNT buckypaper, the CNTs were dispersed in deionized water with Triton X-100 and then sonicated for 1 h. The CNT suspension was filtered through a polytetrafluoroethylene (PTFE) membrane (pore diameter = 0.22 μm) under vacuum and washed with water and methanol to remove any remaining surfactant. The resulting CNT buckypaper was peeled off of the PTFE membrane and dried under vacuum. Neither a polymeric binder nor a conductive agent was used. The active area and loading of the cathode were 0.785 cm^2 and 1.0 mg cm^{-2}, respectively. A porous Ni foam was placed on the cathode side to allow for uniform distribution of O_2 gas as well as efficient current collection. For a comparative study, a cell was assembled using a commercially available LICGC™ SP-01 membrane (thickness ~180 μm, OHARA Inc., Japan). All of the cell components were dried under vacuum at 120 °C for 12 h and directly transferred to an Ar-filled glove box for cell assembly. The cells were placed in a gas-tight chamber with a controlled pressure and gas flow rate, and high-purity O_2 gas was supplied to the chamber. Galvanostatic discharge profiles were measured at a specific current of 50 mA g^{-1} (based on the cathode weight) with a cut-off voltage of 2.0 V vs. Li/Li^+ using a battery tester (WonATech, WBCS3000S). For rate-capability tests, the cell was discharged with a limited capacity of 400 mAh g^{-1} at various specific currents of 50–1,000 mA g^{-1}. After discharging, it was charged using a protocol of constant current (CC)-constant voltage (CV), i.e., CC charge at 50 mA g^{-1} to 4.3 V vs. Li/Li^+ followed by CV charge with a 5 mA g^{-1} cut-off current and a 400 mAh g^{-1} cut-off capacity. For cycling experiments, the cell was discharged with a limited capacity of 400 mAh g^{-1} at 100 mA g^{-1} and was then charged using a CC–CV protocol, i.e., CC charge at 100 mA g^{-1} to 4.3 V vs. Li/Li^+ and CV charge with a 10 mA g^{-1} cut-off current and a 400 mAh g^{-1} cut-off capacity. AC-impedance measurements were conducted at $f = 10^{-2}$–10^6 Hz with an AC signal amplitude of 5 mV using a Bio-Logic SP-200.

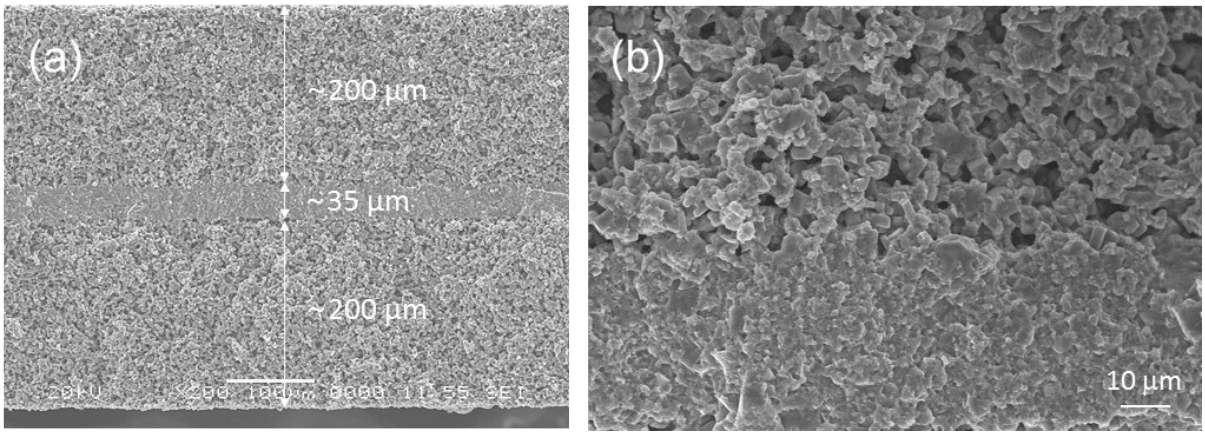

Fig. S1 Cross-sectional SEM micrograph of the sintered triplex-LSSM: (a) low- and (b) high-magnification images.

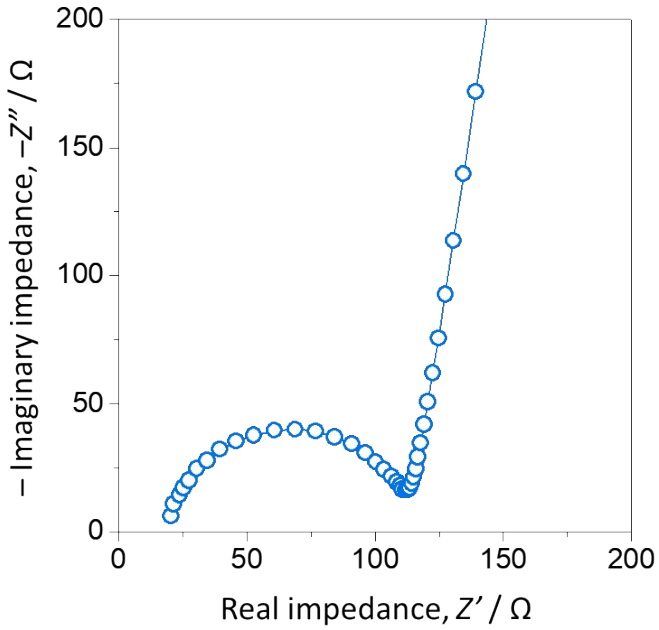

Fig. S2 AC-impedance spectrum of the sintered LATP pellet measured using the Au electrodes.

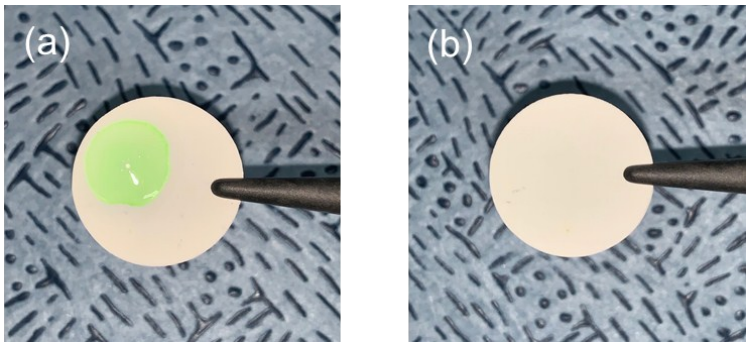

Fig. S3 Photographs showing a test of liquid permeation through the triplex-LSSM. (a) Green-colored liquid was dropped on the one side of the triplex-LSSM, and then, (b) vacuum was applied on the opposite side. No liquid permeation was observed through the triplex-LSSM.

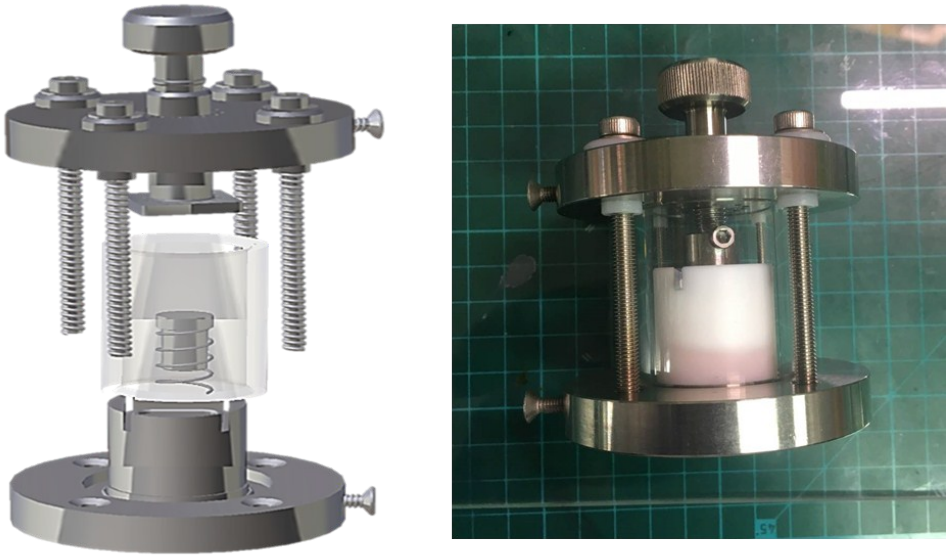

Fig. S4 Two-compartment cell used for electrochemical tests.

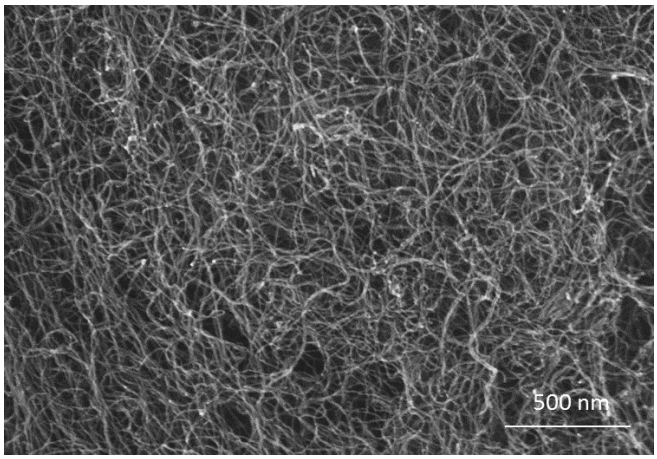

Fig. S5 SEM micrograph of CNT buckypaper.

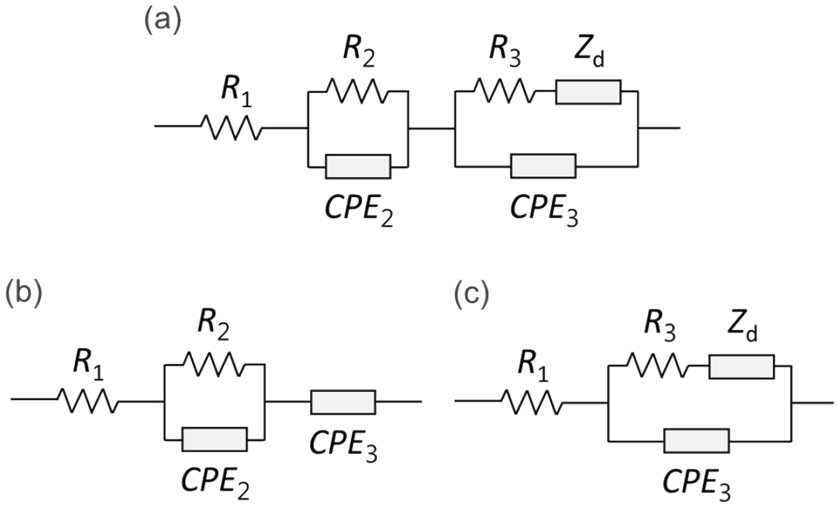

Fig. S6 Equivalent circuits used for fitting of the measured impedance data in (a) Figure 2(c), (b) Figure 2(d), and (c) Figure 2(e). *R*, *CPE*, and Z_d represent the resistance, constant phase element, and diffusion impedance, respectively.

Table S1 Electrical parameters of the LOB with the triplex-LSSM (Figure 2(c)), the triplex-LSSM (Figure 2(d)), and the LOB without the triplex-LSSM (Figure 2(e)) determined from the CNLS fitting of the impedance spectra to the equivalent circuit (Figure S6).

	R_1	CPE_2		R_2	CPE_3		R_3	Z_d		
	(Ω)	C (μF $s^{\eta-1}$)	η (-)	(Ω)	C (μF $s^{\eta-1}$)	η (-)	(Ω)	R_d (Ω)	T (s)	ϕ (-)
LOB with triplex-LSSM	28.6	0.76	0.82	34.2	13.1	0.82	112.1	51.4	0.72	0.5
triplex-LSSM	15.5	0.34	0.88	25.6	10.4	0.84	-	-	-	-
LOB without triplex-LSSM	6.7	-	-	-	44.9	0.83	91.0	42.8	0.59	0.5

$CPE = C(j\omega)^{\eta}$ and $Z_d = R_d \coth([jT\omega]^{\phi}) / ([jT\omega]^{\phi})$

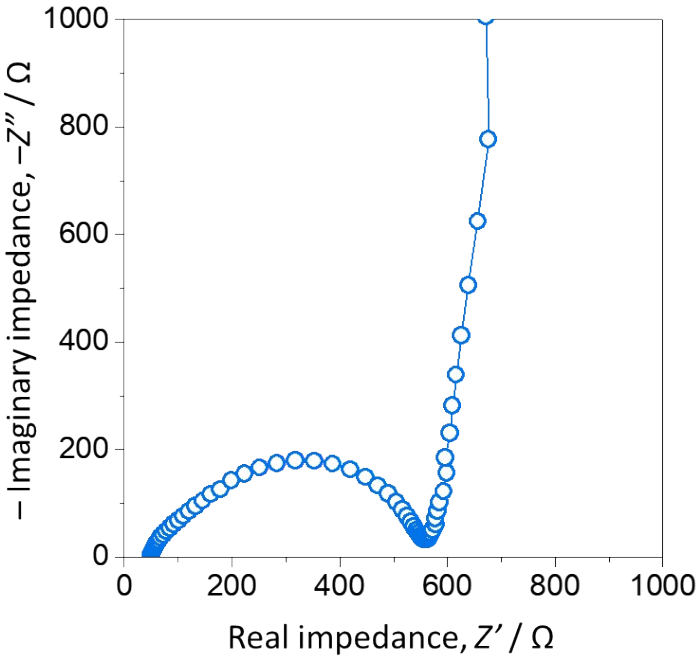

Fig. S7 AC-impedance spectrum of the LOB assembled with LICGC™.

The AC-impedance analysis revealed a higher overall resistance of the LOB with LICGC™ (Fig. S7) compared to the triplex-LSSM-based LOB (Fig. 2(c)). Unlike for the triplex-LSSM-based LOB, the impedance signals associated with Li^+ conduction in LICGC™ and interfacial redox reactions overlapped, which made it difficult to precisely determine the contribution of LICGC™ to the total resistance. Given that the ionic conductivity of the liquid electrolyte (~1×10^{-2} S cm^{-1}) is much higher than that of LATP (1×10^{-4} to 3×10^{-4} S cm^{-1}), we believe that the ion transport in either the porous LATP layer or the cathode separator would not have a dominant influence on the rate-performance.

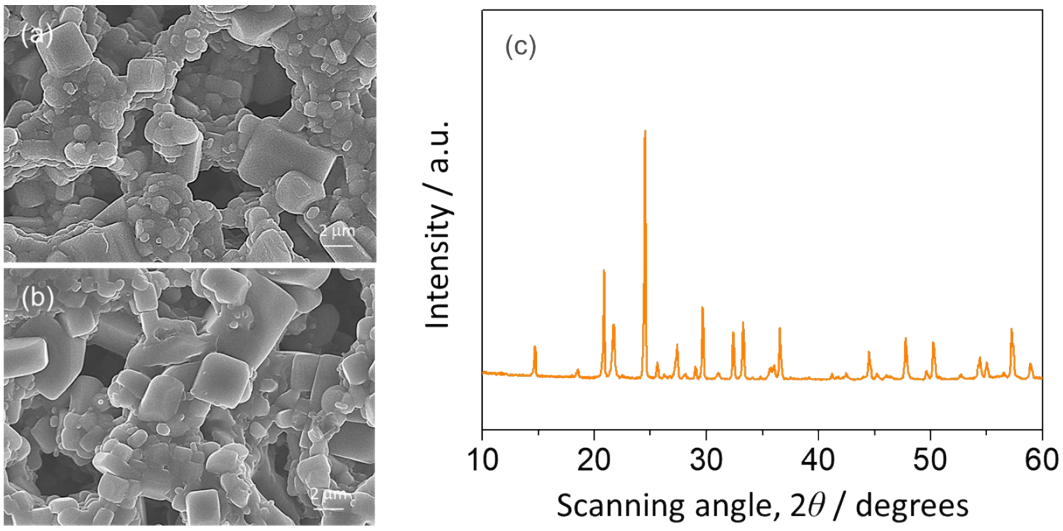

Fig. S8 (a, b) SEM images and (c) XRD pattern of the triplex-LSSM subjected to 40 discharge–charge cycles: (a) exposed to the anolyte (1 M $LiPF_6$ in EC/EMC) and (b) exposed to the catholyte (1 M LiTFSI in TEGDME).

The SEM analysis indicated no microstructural and morphological changes of the triplex-LSSM in contact with the $LiPF_6$- and LiTFSI-containing electrolytes during cycling. Furthermore, the XRD pattern of the triplex-LSSM subjected to 40 cycles appeared almost the same as that of the pristine sample (Fig. 1(e)), indicating that no additional impurity species or secondary phases were formed on the triplex-LSSM after cycling.

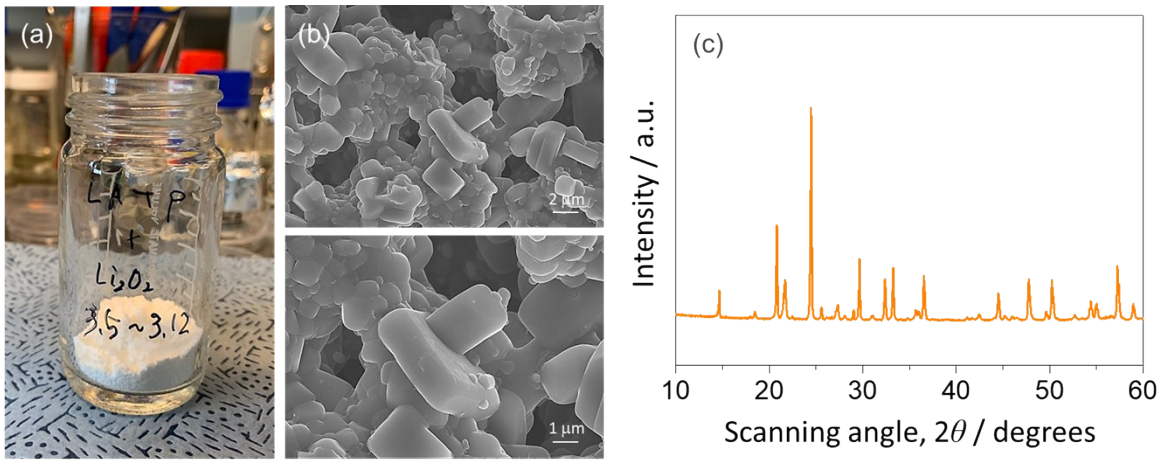

Fig. S9 (a) Photograph showing the storage test of the triplex-LSSM in direct contact with Li_2O_2. (b) SEM images and (c) XRD pattern of the triplex-LSSM subjected to the storage test for 8 days. The storage test was conducted in an Ar-filled glove box.

To further confirm the stability of the triplex-LSSM against chemical attack by the discharge product (Li_2O_2), we stored the triplex-LSSM in direct contact with Li_2O_2 powder (Aldrich) for 8 days (Fig. S9(a)) and then conducted SEM (Fig. S9(b)) and XRD analyses (Fig. S9(c)). The results revealed that any by-products were not formed on the surface and in the pores of the triplex-LSSM.

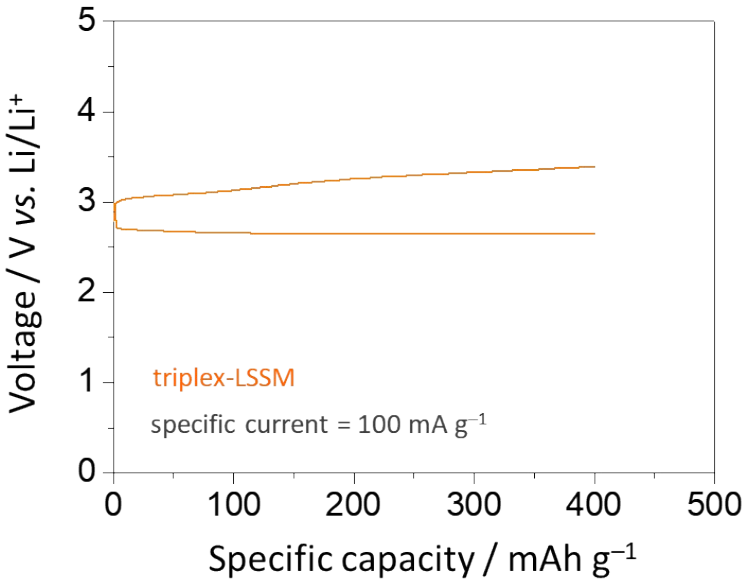

Fig. S10 Typical discharge–charge curve for the LOB with the triplex-LSSM in the presence of LiI as an RM in the catholyte.

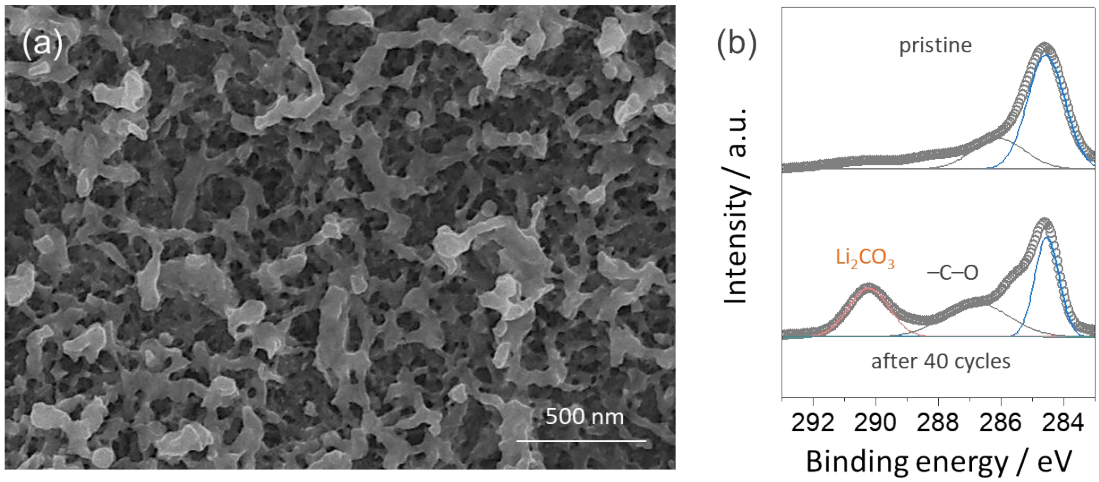

Fig. S11 (a) SEM image and (b) C 1s XPS spectra of the CNT cathode subjected to 40 discharge–charge cycles.

The XPS data of the cycled CNT cathode showed the increased peak intensities for Li_2CO_3 and other C–O species as compared to that of the pristine cathode, which resulted from the parasitic reactions on the cathode due to carbon degradation as well as electrolyte decomposition.